

A comparison between BEM and FEM for elastic registration of medical images

E. Gladilin^{a,*}, V. Pekar^b, K. Rohr^{a,1}, H.S. Stiehl^c

^a University of Heidelberg, IPMB, and DKFZ Heidelberg, TBI, Im Neuenheimer Feld 580, D-69120 Heidelberg, Germany

^b Philips Research Laboratories, Röntgenstr. 24-26, D-22335 Hamburg, Germany

^c University of Hamburg, FB Informatik, AB KOGS, Vogt-Kölln-Str. 30, D-22527 Hamburg, Germany

Received 21 March 2002; received in revised form 30 September 2003; accepted 8 December 2005

Abstract

The aim of medical image registration is to bring different images into the best possible spatial correspondence in order to obtain complementary information for clinical applications. When using physically-based techniques for image registration the transformation of images is typically obtained as the solution of partial differential equations of continuum mechanics. Because of the complexity of real boundary conditions, these equations can usually be solved with the help of numerical techniques only. One standard numerical method is the boundary element method (BEM) which allows to compute the solution exclusively through boundary integration. This paper investigates the applicability of BEM for registration of medical images and quantitatively assesses its advantages and disadvantages in comparison to the previously used finite element method (FEM).

© 2006 Elsevier B.V. All rights reserved.

Keywords: Elastic image registration; Deformable modeling; Boundary element method; Finite element method

1. Introduction

The combination of data from different modalities (for example CT and MR data), the mapping of an image onto an anatomical atlas or the simulation of tissue deformations are important for clinical applications in diagnostics and surgery. In image registration, a transformation which optimally maps all image points of one image onto another image has to be found. Because of the variability of anatomical structures to be registered, rigid transformations are generally not sufficient and non-rigid registration methods have to be applied. One common approach to non-rigid image registration is based on computing elastic transformations which simulate deformations of a solid body under the impact of applied forces [6,9]. Theoretical fundamentals for this approach are provided by elasticity theory, where a linear approximation of the

deformation of physical bodies is described by the Navier partial differential equation (PDE) [1]. A general analytical solution to the Navier-PDE does not exist. However, it can be solved numerically by applying a standard technique for solving PDEs, the finite element method (FEM), which is arbitrarily exact, but also relatively time consuming [7,10]. Others use finite differences for numerical approximation which is not as flexible as FEM [8].

In this paper, we apply an alternative standard numerical method, the boundary element method (BEM), for the registration of medical images and compare it with FEM. BEM allows to find a solution for given boundary value problems exclusively through boundary integration. This has the advantage that only the boundary of the domain of interest has to be discretized, and therefore the dimension of the resulting linear system of equations in BEM is significantly smaller than in FEM. On the other hand, the stiffness matrix of the classical BEM is in general fully occupied and non-symmetric, which complicates the application of efficient solving methods. The existing literature gives no indication about which of the two methods should be used neither for a specific problem, nor in general [14]. In this paper, we introduce for the first time a BEM approach for elastic registration of medical images. In addition, we perform a comparison of the BEM approach with an FEM approach and

* Corresponding author. Address: German Cancer Research Center (DKFZ), Theoretical Bioinformatics, Im Neuenheimer Feld 580, D-69120 Heidelberg, Germany. Tel.: +49-6221-423604.

E-mail address: e.gladilin@dkfz.de (E. Gladilin).

¹ This work has been carried out while E. Gladilin, V. Pekar, and K. Rohr have been with the University of Hamburg, FB Informatik, AB KOGS [12].

provide qualitative and quantitative results using both synthetic and real images.

The paper is organized as follows. First, we briefly describe some necessary fundamentals of elasticity theory as well as numerical techniques for solving linear elastic boundary value problems, i.e. FEM and BEM. Then, experimental results of elastic registration using BEM, as well as a quantitative comparison of the performance between BEM and FEM are presented.

2. Elasticity theory and numerical solving methods

In elasticity theory, physical bodies are described as continua. Under applied forces physical bodies are deformed, which means that they change both their shape and volume. The inner stresses counteract the applied forces. Using a linear approximation, we have the following relations between the strains u_{ik} (resp. displacements u_i), the stresses σ_{ik} (resp. normal stresses or tractions t_i) and the applied force density F_i

$$\text{Equilibrium equation : } \sigma_{ik,k} = -F_i, \tag{1}$$

$$\text{Hook's law : } \sigma_{ik} = \frac{E}{1+\nu} \left(u_{ik} + \frac{\nu}{1-2\nu} u_{ll} \delta_{ik} \right), \tag{2}$$

$$\text{Navier-PDE : } \Delta \vec{u} + \frac{1}{1-2\nu} \text{grad div } \vec{u} = -\frac{2(1+\nu)}{E} \vec{F}, \tag{3}$$

where E denotes the Young modulus and ν is the Poisson ratio. Using Eq. (3) for image registration, the transformation of all image points with coordinates x_i in the source image is completely described if the displacements u_i are known

$$x'_i = x_i + u_i, \tag{4}$$

where x'_i are the new coordinates of the transformed image points. The aim of elastic registration is to solve the Navier-PDE Eq. (3) for given boundary conditions. In practice, because of the complexity of given problems it is generally impossible to find analytical solutions. Numerical solutions are usually computed as a linear combination of independent functions ϕ_k

$$u' = \sum_{k=1}^N u_k \phi_k, \tag{5}$$

where the unknown coefficients u_k have to be found. Let u be the exact solution of the linear PDE $L_u = b$, where L is a linear differential operator. The so-called ‘residual’ or ‘error function’ $R = L_u - b$ is equal to zero for the exact solution u and, in general, different from zero for an approximative solution u' . The errors are forced to be zero in a certain average sense, and this is done differently for each particular method. Several well-known techniques are based on the so-called method of weighted residuals (MWR), e.g. FEM and BEM. In this case, the integral over the error R weighted with functions

ψ_k is set to zero:

$$\int_{\Omega} R \psi_k d\Omega = 0. \tag{6}$$

The function ψ_k is denoted as weighting functions and determines how the error R is distributed over the domain Ω .

3. The finite element method

The general approach in FEM consists of the following steps [3]: (i) The domain Ω is subdivided into a finite number of elements. (ii) All relevant quantities are approximated for each element through locally defined functions and are incorporated into Eq. (6). If the weighting functions in Eq. (6) are the same as the functions ϕ_k in Eq. (5), this variant of MWR is called the Galerkin-method. (iii) Using Eq. (6) together with boundary conditions, a linear system of equations results with the node-variables u_k

$$\mathbf{K} \mathbf{u} = \mathbf{b}, \tag{7}$$

where \mathbf{u} is the vector of the unknown coefficients u_k , \mathbf{b} is the load vector and \mathbf{K} is the so-called stiffness matrix. The stiffness matrix contains all integrals and material parameters, is typically very large, and has a band structure, i.e. it is filled with zeros except the entries close to the main diagonal. FEM has been applied to elastic image registration, for example, in [7,10,11].

4. The boundary element method and its implementation

4.1. Basics of the linear elastic BEM

The main advantage of BEM in comparison to FEM is that one only needs to discretize the boundary of the domain in order to compute the solution for the whole domain. Formally, the domain integrals are transformed into boundary integrals. In comparison to FEM, where the weighting functions are defined locally, the weighting functions in BEM are defined globally. In the latter case, these functions are the so-called fundamental solutions of the Navier-PDE, i.e. the solutions in the case of a Dirac-distributed force and an infinitely extended elastic medium. The sampling property of the Dirac function is exploited to obtain the solution in the whole domain exclusively using boundary integrals [2]

$$u_i(P) = \int_{\Gamma} \left[u_{ij}^*(P,Q) t_j(Q) - t_{ij}^*(P,Q) u_j(Q) \right] ds, \tag{8}$$

where $P \in \Omega$ is an arbitrary point within the domain, $Q \in \Gamma$ is a boundary point, u_{ij}^* and t_{ij}^* are the fundamental solutions of the Navier-PDE for the displacements and tractions, respectively. The so-called Somigliana identity Eq. (8) allows to compute displacements $u_i(P)$ in the domain Ω when boundary displacements $u_j(Q)$ and tractions $t_j(Q)$ are known. Since boundary conditions are usually given only in the form of prescribed displacements, one has no information about

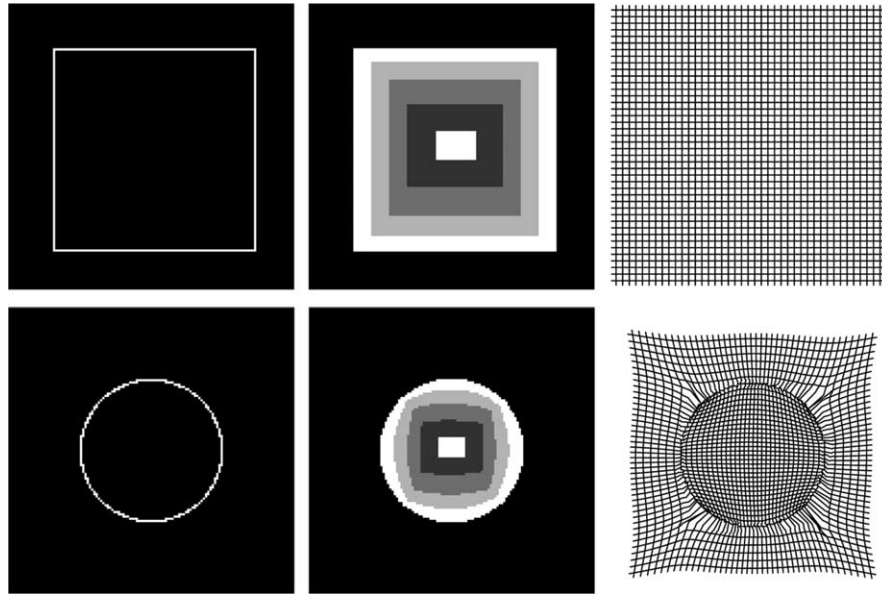


Fig. 1. Top row, from left to right: boundary of the source image, source image, image grid. Bottom row: boundary of the target image, deformed image, deformed image grid.

boundary tractions. However, the tractions can be obtained from the Somigliana identity Eq. (8) when applying this equation to the boundary ($P, Q \in \Gamma$). In all other respects, the general approach in BEM is the same as in FEM. After discretization of the boundary, all relevant quantities are approximated as in Eq. (5) and incorporated into Eq. (8). Finally, one obtains a linear system of equations w.r.t. the node variables

$$\mathbf{H}\mathbf{u} = \mathbf{G}\mathbf{t}. \quad (9)$$

here, \mathbf{H} and \mathbf{G} are the so-called hypermatrices which imply the corresponding boundary integrals and material constants, \mathbf{u} and \mathbf{t} are the vectors of the node displacements and tractions, respectively. The unknown node tractions can simply be obtained from the known displacements by solving Eq. (9) w.r.t. \mathbf{t} : $\mathbf{t} = \mathbf{G}^{-1}\mathbf{H}\mathbf{u}$.

4.2. Implementation details

In the implementation of BEM, the following points require particular attention (we consider for simplicity only 2D case, however, most of the issues below are also valid in 3D):

1. Weighting functions in the BEM (the fundamental solutions) are defined globally. Consequently, all nodes of the boundary network are coupled with each other and the resulting system matrices \mathbf{H} and \mathbf{G} are, in general, fully occupied and non-symmetric in a difference to the sparse and symmetric matrices in FEM.
2. Depending on the dimension of the given problem, the fundamental solutions have a singularity of type r^{-n} or $\log(r)$. This causes a divergence of the numerical solution for $r \rightarrow 0$ which is known as the typical BEM failure near boundaries (see also Section 5.1 below).
3. In order to assembly the linear system of equations, singular

integrals must be computed. This can be done only numerically at the expense of efficiency.

4. With the image raster, a network of nodes for BEM is explicitly given. Unfortunately, the 2D boundary resulting from the ad-hoc parametrization on the basis of raster nodes is not smooth. This has far reaching consequences for BEM: the tractions on the non-smooth boundary are unsteady, which in turn requires additional efforts for the discretization, i.e. the application of the node duplication technique, and also leads to non-square stiffness matrices. In this paper, we assume steady tractions, which premise a smooth boundary. To satisfy this requirement, the boundary has to be smoothed, for example by using a Fourier-expansion [4] as in our case.

The implementation of BEM consists of the following steps:

- extraction and parametrization of the boundary of the source and target object, for example by using an edge detection operator,
- derivation of correspondences between the source and target boundary outlines, for example by using deformable models or minimal-distance algorithm,
- computation of displacements for all image points by solving Eqs. (8) and (9).

5. Experimental results

We have implemented the linear elastic BEM approach for elastic image registration under Khoros [13] in C. For the FEM approach, we used an existing implementation on the same software platform [10]. In this section, the experimental results of image registration via BEM in conjunction with a quantitative comparison with FEM are presented.

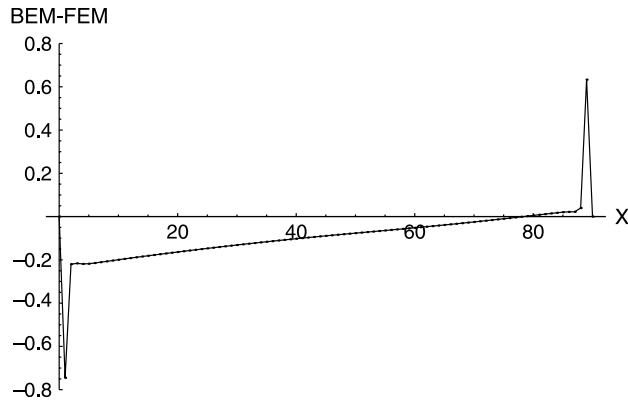


Fig. 2. Difference between the BEM and the FEM computed displacement vectors (in pixels). The largest deviations of the BEM solution from that of FEM arise due to the singularity of the fundamental solution near the boundary ($X=0$ and 90). However, as can be seen these deviations are smaller than one pixel.

5.1. Comparison of the registration accuracy

In the first experiment, we analyzed synthetic images. A square has been transformed into a circle (see Fig. 1).

In this example, the boundaries have not been smoothed for the BEM approach, since with the exception of the four corner points of the square the boundary is already smooth. Boundary correspondences have been computed by making the boundary of the square act like a ‘snake’ [5]. The registration result using FEM has been obtained by applying the method from [10]. In order to be able to compare the displacement fields (\vec{u}_{BEM} vs. \vec{u}_{FEM}) quantitatively, we calculated the average relative difference (ARD) and its standard deviation (σ_{ARD}) as

$$\text{ARD} = \frac{1}{N} \sum_i^N \frac{|\vec{u}_{\text{BEM}}(i) - \vec{u}_{\text{FEM}}(i)|}{\min(|\vec{u}_{\text{BEM}}(i)|, |\vec{u}_{\text{FEM}}(i)|)}, \quad (10)$$

$$\sigma_{\text{ARD}} = \sqrt{\frac{\sum_i^N \left(\frac{|\vec{u}_{\text{BEM}}(i) - \vec{u}_{\text{FEM}}(i)|}{\min(|\vec{u}_{\text{BEM}}(i)|, |\vec{u}_{\text{FEM}}(i)|)} - \text{ARD} \right)^2}{N-1}}, \quad (11)$$

where N is the number of domain points. For the image in Fig. 1 the following values have been obtained: $\text{ARD}=0.016515$, $\sigma_{\text{ARD}}=0.036729$. This means that the displacement field computed with BEM deviates in average up to about 5% ($\text{ARD} + \sigma_{\text{ARD}}$) from the result obtained by FEM. In Fig. 2, the absolute difference between the displacement vectors (BEM – FEM) along a horizontal line through the middle of the square (middle of top row in Fig. 1) is shown. The largest deviations of the BEM solution from that of the FEM arise due to the singularity of the fundamental solution near the boundary ($X=0$ and 90). However, it can be seen that these deviations are smaller than one pixel.

For the tests with clinical images, MR-slices of the human brain have been used. The boundary outline (top left in Fig. 3) was extracted by applying a Canny edge operator to the source image (top right) and smoothing it by using a 2D Fourier expansion, see [4]. In this example, the task is to map the source image boundary to an ellipse (bottom left) and to transform the remaining areas accordingly. The correspondences were derived by using a minimal distance algorithm. As one can see in Fig. 3, the results of the computation with BEM and FEM visually correspond well.

5.2. Comparison of the efficiency

In order to compute a numerical solution by using BEM, one needs to discretize only the boundary. Thus, the linear system of equations is one dimension smaller compared to that of FEM. Consequently, the matrices in BEM require significantly less memory. On the other hand, the matrices in BEM are in

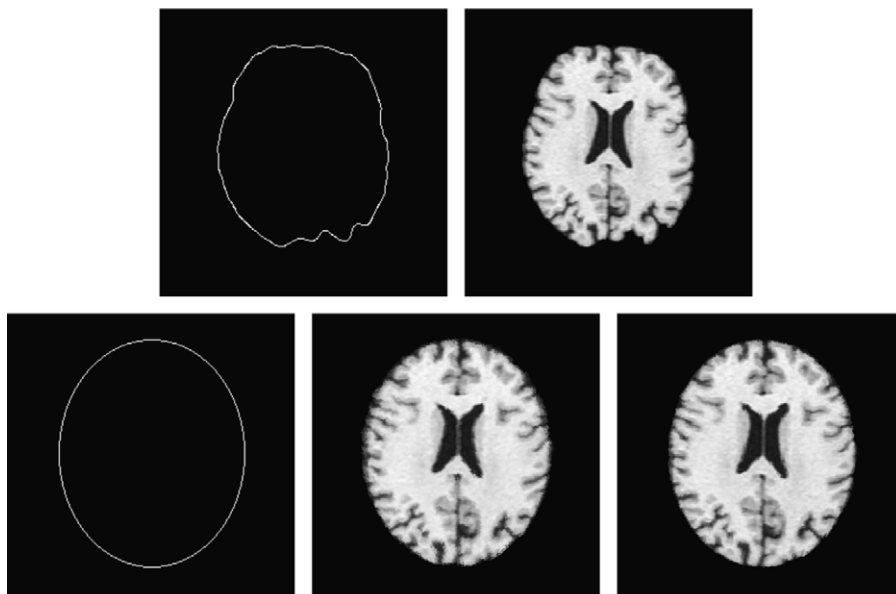


Fig. 3. Top: source image (right) and its boundary outline (left). Bottom: target image boundary outline (left), result of applying the BEM approach (middle) and the FEM approach (right).

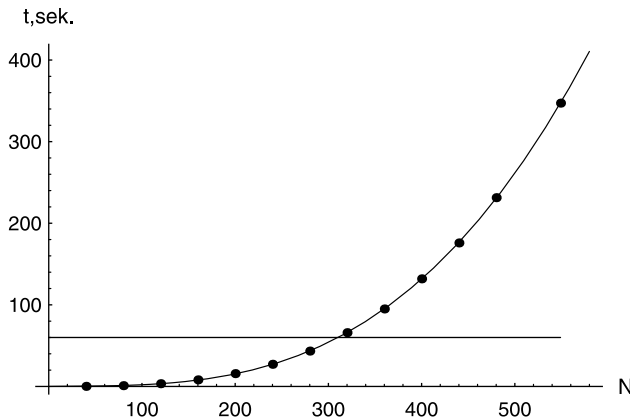


Fig. 4. Computation time (in seconds) for the BEM approach to compute the matrix \mathbf{G}^{-1} by using the Gauss elimination algorithm as a function of the number of the boundary points N . The straight line ($t=60$) corresponds to the computation time using FEM for a 256×256 image.

general fully occupied and non-symmetric in comparison to the sparse and symmetric matrices in FEM. Therefore, efficient techniques for solving linear systems of equations with sparse and symmetric matrices as used in FEM, e.g. the method of conjugate gradients, cannot be applied in BEM. Instead, we used the Gauss elimination algorithm which proved to be relatively time consuming.

The dimension of the matrix \mathbf{G} in Eq. (9), which has to be inverted, is $(2 \times N_R)^2$, where N_R denotes the number of boundary points. For the 128×128 synthetic image in Fig. 1, $N_R=360$ and the dimension of \mathbf{G} is $(2 \times 360)^2=518400$. On a SUN-Ultra II workstation the matrix inversion took 1 min 35 s. The total computation time for this image amounted to 3 min. The computations for the 256×256 image with $N_R=548$ took approx. 9 min, thereof 5 min 47 s only for the inversion of the fully occupied matrix of $(2 \times 548)^2$ elements. The computation time for the same image using FEM with quadratic elements corresponding to the image raster took 56 s for a sparse matrix of $(2 \times 256 \times 256)^2$, see Fig. 4.

6. Conclusion

We have introduced the boundary element method for elastic image registration and compared it with FEM. BEM allows to solve a registration problem exclusively through boundary integration. Thus, only the boundaries of the region of interest have to be discretized. The resulting linear system of equations in BEM is one dimension smaller than that of FEM. Application of BEM for the registration of 2D images has shown that good qualitative as well as quantitative results can

be achieved in comparison to FEM. In 2D, even if no adaptive domain discretization is carried out and the whole image raster used as a mesh, FEM appears to be more efficient for image registration than the classical BEM. In addition, mesh generation in 3D requires incomparably more efforts than in 2D. However, recent BEM formulations, e.g. symmetric Galerkin BEM (SGBEM) [15], indicate that they become more computationally efficient. Hence, we see a potential for further application of BEM in elastic registration.

References

- [1] L.D. Landau, E.M. Lifschitz, *Lehrbuch Der Theoretischen Physik, Band 7, Elastizitätstheorie*, Akademie-Verlag, Berlin, 1989.
- [2] D.E. Beskos, *Boundary Element Methods in Mechanics*, Elsevier, Amsterdam, 1987.
- [3] H.R. Schwarz, *Methode der finiten Elemente*, B.G. Teubner, Stuttgart, 1991.
- [4] D.H. Ballard, C.M. Brown, *Computer Vision*, Prentice-Hall, London, 1982.
- [5] M. Kass, A. Witkin, D. Terzopoulos, Snakes: active contour models, *International Journal of Computer Vision* 1 (4) (1988) 321–333.
- [6] R. Bajcsy, S. Kovačič, Multiresolution elastic matching, *Computer Vision, Graphics, and Image Processing* 46 (1989) 1–21.
- [7] J.C. Gee, D.R. Haynor, M. Reivich, R. Bajcsy, Finite element approach to warping of brain images, in: M.H. Loew (Ed.), *Proceedings of the SPIE 2167, Medical Imaging 1994: Image Processing*, 15–18 February, Newport Beach, CA, USA, 1994, pp. 327–337.
- [8] G.E. Christensen, M.I. Miller, M. Vannier, U. Grenander, Individualizing neuroanatomical atlases using a massively parallel computer, *IEEE Computer* 29 (1) (1996) 32–38.
- [9] C. Davatzikos, Spatial transformation and registration of brain images using elastically deformable models, *Computer Vision and Image Understanding, Special Issue on Medical Imaging* 66 (2) (1997) 207–222.
- [10] W. Pekar, C. Schnörr, K. Rohr, H.S. Stiehl, Parameter-free elastic deformation approach for 2D- and 3D-registration using prescribed displacements, *Journal of Mathematical Imaging and Vision* 10 (2) (1999) 143–162.
- [11] A. Hagemann, K. Rohr, H.S. Stiehl, U. Spetzger, J.M. Gilsbach, Biomechanical modeling of the human head for physically-based, non-rigid image registration, *IEEE Transactions on Medical Imaging* 18 (10) (1999) 875–884.
- [12] E. Gladilin, W. Pekar, K. Rohr, H.S. Stiehl, Vergleich der Randelemente mit der Finite-Elemente-Methode zur elastischen Registrierung medizinischer Bilder, Technical Report FBI-HH-M-287/99, FB Informatik, Universität Hamburg, June 1999.
- [13] Khoros—Integrated Development Environment, <http://www.khoros.com>.
- [14] M. Clerc, A. Dervieux, R. Keriven, O. Faugeras, J. Kybic, T. Papadopoulo, Comparison of BEM and FEM Methods for the E/MEG Problem, in: *Proceedings of the Biomag2002*, Jena, Germany, August 2002.
- [15] S. Miccoli, Efficient solution of symmetric systems of algebraic equations arising from Galerkin boundary element discretizations of 3D elastostatics problems, in: *Proceedings of the IABEM 2002*, Austin, USA, May 2002.